State-of-Grid based Control of DC Microgrids: A Communication-Free Solution

Ömer Ekin[1], Max Leuthaeusser[1], Giovanni De Carne[1], and Veit Hagenmeyer [1]

[1]Affiliation not available

October 02, 2024

Abstract

DC Microgrids are advantageous solutions for integrating renewable energy sources. Existing control methods rely on communication, which can be unreliable. To address this, a novel State-of-Grid (SoG) based control is proposed. In order to address this challenge, after defining the notion of State-ofGrid (SoG), the present paper introduces a novel SoG based control for DC Microgrids. The proposed approach ensures a communication-free operation of DC Microgrids, capable of power and load sharing while balancing the State-of-Charge (SoC) of each Energy Storage System (ESS). In this SoG based control, the ESS converters are fully decentralized controlled to map the SoC of each BESS into a corresponding output voltage range. This streamlined approach significantly simplifies SoC equalization and power-sharing without necessitating dedicated communication infrastructure. The proposed approach encompasses both the AC-coupled mode and the islanded mode. Moreover, through this SoG based control, completely communicationfree balancing of the SoCs throughout AC and DC Microgrids is achieved. The proposed approach is implemented and validated using a DC Microgrid experimental setup comprising two ESS, Photovoltaic (PV) arrays, multiple loads at different voltage levels, and a DC-AC interlink converter allowing power exchange with an AC Grid. Both islanded and AC-coupled mode experiments are examined.

State-of-Grid based Control of DC Microgrids: A Communication-Free Solution

Ömer Ekin, *Graduate Student Member, IEEE*, Max Leuthaeusser, *Student Member, IEEE*, Giovanni De Carne,*Senior Member, IEEE*, Veit Hagenmeyer, *Member, IEEE*

***Abstract*—DC Microgrids are advantageous solutions for integrating renewable energy sources. Existing control methods rely on communication, which can be unreliable. To address this, a novel State-of-Grid (SoG) based control is proposed. In order to address this challenge, after defining the notion of State-of-Grid (SoG), the present paper introduces a novel SoG based control for DC Microgrids. The proposed approach ensures a communication-free operation of DC Microgrids, capable of power and load sharing while balancing the State-of-Charge (SoC) of each Energy Storage System (ESS). In this SoG based control, the ESS converters are fully decentralized controlled to map the SoC of each BESS into a corresponding output voltage range. This streamlined approach significantly simplifies SoC equalization and power-sharing without necessitating dedicated communication infrastructure. The proposed approach encompasses both the AC-coupled mode and the islanded mode. Moreover, through this SoG based control, completely communication-free balancing of the SoCs throughout AC and DC Microgrids is achieved. The proposed approach is implemented and validated using a DC Microgrid experimental setup comprising two ESS, Photovoltaic (PV) arrays, multiple loads at different voltage levels, and a DC-AC interlink converter allowing power exchange with an AC Grid. Both islanded and AC-coupled mode experiments are examined.**

***Index Terms*—DC Microgrid, Battery Energy Storage System (BESS), Decentralized Control Strategy, State-of-Grid (SoG), SoC-balancing, Power Management.**

I. Introduction

THE increasing integration of Renewable Energy Sources (RES) and electric vehicles calls for an enhancement of the electrical grid. The vast majority of RES generate direct current (DC) or require an intermediate DC circuit, and thus need to be connected to the public distribution grid via power electronics. On the other hand, energy storage systems and a significant portion of electrical consumers convert alternating current (AC) back to DC for utilization. The advantages of DC Microgrids, include fewer converters resulting in reduced semiconductor usage and costs, higher efficiency and reliability due to fewer conversion steps, decreased copper conductor requirements resulting from the absence of reactive power and skin effect, enhanced modularity and scalability due to the absence of frequency and synchronization constraints, and reduced harmonic distortion, and their intrinsic recuperation capability of all connected AC loads highlight their superiority in modern power systems. For this reason, integrating RES and storage technologies into the distribution grid via DC Microgrids has emerged as a promising solution and has become the focus of research [1], [2]. While the primary control objective of DC Microgrids is to regulate the bus voltage within a desired range, other essential control objectives are indispensable for the implementation of practical DC Microgrids. These include power sharing capabilities, State-of-Charge (SoC) equalization, and the provision of ancillary services between the Microgrid and an AC Grid [3], [4]. SoC equalization is a critical issue in Microgrids due to the lifespan of batteries, particularly when managing multiple EES in the same network. If the batteries are charged prematurely, the available charging capacity in the grid decreases. In case of over-production of RES, the remaining uncharged batteries must charge at high power, resulting in reduction of their operational efficiency and lifespan. Therefore, effective coordination to eliminate discrepancies in SoC among the batteries is crucial. SoC balancing enhances reliability, maximizes energy utilization, and prevents energy losses in situations of excess generation due to reduced charging capacity resulting from the premature completion of charging in some batteries [5].

In hierarchical control based approaches high-frequency communication is required for steady and dynamic power sharing capability [6]. Such communication requirement in an energy grid increases inevitably complexity and costs. In addition, communication technology brings new challenges

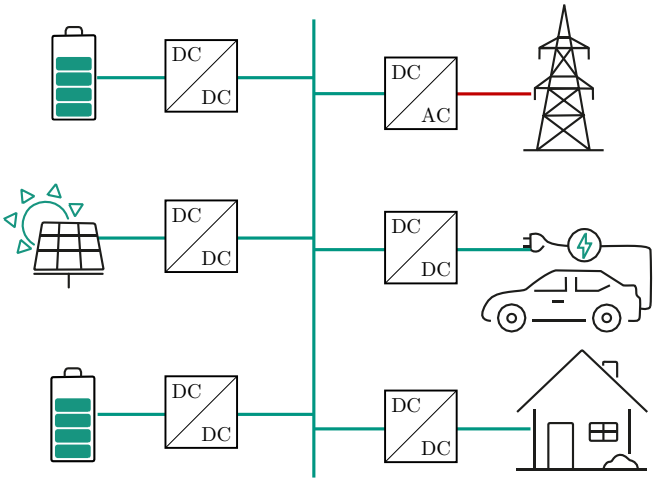

Fig. 1. Schematical block diagram for a DC Microgrid architecture

This work has been supported by the Helmholtz Association under the program "Energy System Design" and under the Helmholtz Young Investigator Group "Hybrid Networks" (VH-NG-1613).

such as vulnerability to cyber-attacks, reliability concerns, compatibility issues, privacy and data security risks, regulatory compliance requirements, maintenance challenges, and dependency on external networks [7]. Decentralized approaches, on the other hand, operate based on local measurements, thereby bypassing the drawbacks of communication based methods. For instance, droop based control [8] can achieve power sharing capability without communication, however, they have to make a compromise between voltage regulation and load sharing. The present paper proposes a novel control method that can handle SoC balancing, includes a self-regulating effect for resistive loads, and enables a synergistic AC-coupling, allowing the DC-AC interlink converter to autonomously manage the power flow between an AC grid and its DC side. Furthermore, by mapping the DC bus voltage and AC grid frequency into representative quantities called State-of-Grid (SoG) a novel SoG based DC-AC interlink control strategy is introduced, that allows decentralized bidirectional grid support between both grids. The predetermined maximum deviation between the reference voltage and the DC bus voltage ensures reliable coordinated operation between DC and the AC grid.

The main contribution of this work is a control method that enables

(1) SoC balancing, allowing each SoC within the entire grid to equalize without additional communication.
(2) Synergistic DC-AC Coupling, allowing the interlink converter to support both grids according to the requirements.
(3) Power sharing capability, even with different line resistances among the BES.
(4) Inherent tertiary control interfaces for optimization, through tertiary control using the setpoints.

The paper is organized as follows: In Section II, a comprehensive review of state-of-the-art methodologies is presented. In Section IV the DC Microgrid configuration and components are explained. The proposed control strategy is explained in Section III. In Section V, the performance of the proposed control strategy is demonstrated through a real DC Microgrid experimental setup. Finally, a conclusion is given in Section VI.

II. State-of-Art SoC balancing

In order to emphasize the novelty of this work, in this section, a review of the prevailing methodologies within the realm of SoC balancing and voltage-Frequency Mapping is presented and compared with this work's contributions. In [22], gain scheduling is employed to adjust controller gains based on load conditions, thereby enhancing voltage regulation and load-sharing performance. However, it is noteworthy that Gain Scheduling methods in Microgrids are constrained to proportional controllers [23]. In [9], the gain scheduling method is modified by using fuzzy control; in this way, the SoC and output power of each EES are gradually balanced. However, a change in the grid, such as adding or removing battery storage, requires communication within the network [9]. In [10], the output power of each ESS is designed to be proportional to its corresponding SoC; however, only the discharge process is considered. In [11] this approach has been extended to include the charging process. These SoC droop based methods do not rely on communication but require all batteries to have the same capacity. Also in [12], an adaptive SoC based droop considering different batteries with different specifications and capacities. The approach is only validated by simulation. In [13], a power sharing approach is presented to balance the SoC among BESSs in a DC Microgrid. However, this approach requires a communication network to exchange system data. In [17], the reference voltage for various BESSs is dynamically adjusted based on their SoC to achieve SoC balancing. However, this approach does not include synergistic AC-coupling. In [21], a communication-free power management strategy is proposed for islanded DC microgrids. This strategy achieves state-of-charge (SoC) balancing among different energy storage units (ESUs) by adjusting droop coefficients according to varying SoC conditions. None of the aforementioned approaches [7]–[11] and also [22], [23] considered the coordination between the DC Microgrid and the distribution grid. In [14], power sharing between the DC and AC sides of a hybrid Microgrid is achieved by enforcing the normalized equality between AC frequency and DC voltage with an interlink converter. However, this results in

TABLE I
State of the Art Comparison

References	Focus	Communication free	SoC-balancing	Load sharing	Synergistic AC-coupling	HW validated
[9]	Fuzzy logic with SoC based Gain scheduling	✓	(✓)	×	×	✓
[10], [11]	SoC based droop	✓	✓	×	×	✓
[12]	SoC based droop	✓	✓	✓	×	×
[13]	Virtual power rating	(✓)	✓	×	×	✓
[14], [15]	Normalized droop AC-DC interlink	✓	×	×	✓	✓
[16]	Normalized droop AC-DC interlink	✓	×	✓	✓	✓
[17]	DC bus voltage signaling	✓	✓	×	×	✓
[18]	AC superimposed on DC voltage to modify droop	✓	×	×	✓	✓
[19]	Filter based Decentralized Control	✓	✓	×	×	×
[20]	Master/Slave bus voltage	✓	✓	✓	(✓)	(✓)
[21]	Adaptive droop	✓	✓	✓	×	✓
The present paper	Flexible DC voltage SoG based control	✓	✓	✓	✓	✓

the interlinking converter operating almost constantly during load fluctuations, which amplifies the power dissipation within the converter. To reduce this operating loss, [15] proposes a progressive tuning of the power flow using energy storage. Also in [16], a distributed power flow control and management operating on both AC and DC. Using a two-stage modified droop method for the bidirectional power control of the interlink converter during different operation modes of the hybrid AC/DC Microgrid.

However, approaches [14]–[16] do not include SoC balancing, as well as in [18], in which an AC voltage is superimposed on the nominal DC voltage to modify the conventional droop control. Furthermore, none of the approaches consider grid-supporting load capability. In [20], an SOC based control method is presented that is tailored to grid-connected DC Microgrids. The dynamics of the AC grid are not considered. The utility grid is activated or deactivated based on the requirements of the DC grid, resulting in voltage fluctuations during transitions in grid connection status that impact the operational stability of the DC Microgrid. Additionally, support towards the AC grid is not addressed.

Tab. I summarizes the different approaches based on a literature review as referenced. Synergistic AC-coupling refers to a bidirectional grid-supportive functionality of the interlink converter. Check marks in brackets are considered to be partially fulfilled. For example, if Hardware (HW) experiments were only carried out with very low power levels, they are deemed insufficient for real HW applications. It can be concluded, that the existing works do not include all the features proposed in the present work, such as being communication-free, fostering SoC balancing, actively influencing the load, coupling with the AC grid, and being experimentally validated. It is important to clarify that while some works may not explicitly demonstrate certain aspects, this does not necessarily imply an inherent inability of the methods to support those functions. Our conclusions regarding these methods are based on the available evidence and are framed within the context of the demonstrated capabilities and limitations as presented in the literature.

III. Proposed SoG based Droop Control Method

This section introduces the basic concept for the State-of-Grid based approach. Each ESS is connected to the DC Microgrid through a DC/DC-converter as illustrated in Fig. 1. The DC voltage can be mapped to a representative quantity (referred to here as SoG) in a steady state, and it can be used in an equivalence relationship with the frequency to regulate the DC/AC converter. Analogous to the grid frequency, which serves as an indicator of overproduction or under-production of electrical energy in the AC network, the voltage in the DC network becomes an indicator through the approach developed here. This makes it possible to control the DC/AC converter in such a way that it regulates a relative deviation between the SoGs to zero. This ensures that the DC Microgrid and the AC grid will be controlled to maintain the same state. The control scheme is depicted as exemplary for all four components in Fig. 2. The SoG based method is controlling the DC Microgrid side output voltage of these DC/DC converters depending on the SoC of the batteries. The higher the SoC, the higher the target voltage. Since the converters are all connected in parallel to the DC Microgrid, a higher target voltage than the grid side voltage will result in a current flow, and thus also a power flow, towards the grid. Conversely, the opposite holds for target voltages lower than the grid voltage. This control method enables inherent SoC equalization for the DC Microgrid.

A. Proposed SoC-V based droop

The proposed SoC-V droop is implemented using:

$$V^*_{C,Bi} = V^*_{DC} \cdot \kappa_i \tag{1}$$

$$\kappa_i = 1 + \sigma \frac{SoC_i - SoC^*_i}{SoC_{\Delta,i}} \tag{2}$$

where $V^*_{C,Bi}$ is the controlled output voltage of the converter of battery $i \in \{1, 2\}$ and $\kappa_i \in [\kappa_{min}, \kappa_{max}]$ is a scaling factor based on the respective State-of-Charge.

V^*_{DC} is the desired DC bus voltage in the steady state. $SoC_i, SoC^*_i \in [0, 1]$ are the measured and the desired SoC of the battery i. The $SoC_{\Delta,i}$ is defined as:

$$SoC_{\Delta,i} = \begin{cases} SoC^{\max} - SoC^*_i, & \text{if } SoC_i - SoC^*_i > 0, \\ SoC^*_i - SoC^{\min}, & \text{otherwise.} \end{cases} \tag{3}$$

with $\sigma \in [0, 1]$ as the allowed deviation (e.g. $\sigma = 0.05$ if 5% variation allowed). By applying the mapping (1)-(3), an inherent SoC equalization is achieved. This method allows the SoC of individual batteries to be freely chosen by adjusting the setpoint values SoC^*_i. This can be done, for example, through tertiary control or manually. The case differentiation made by Eq. (3) ensures that the range is always divided across the adjustment range, regardless of the setpoint. However, there is still a significant reaction when setpoints are chosen near the limits. This is illustrated in Fig. 3. This mapping results in a steeper slope in the descending direction in the case of an SoC setpoint SoC^*_L near the minimum SoC, making it more difficult to reach the minimum SoC. Conversely, it leads to a gentler slope in the ascending direction for an SoC

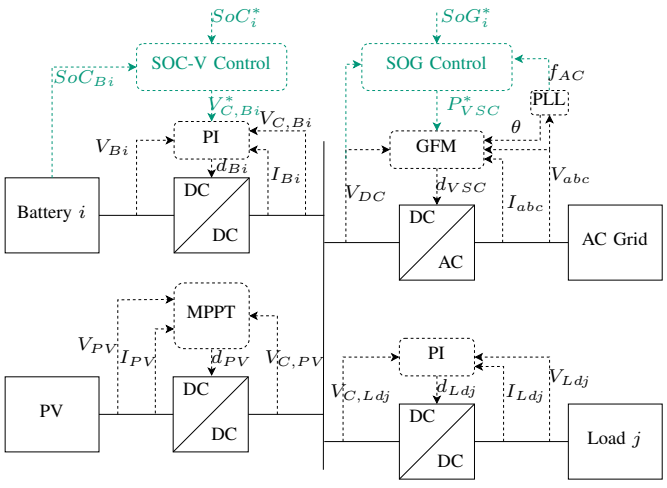

Fig. 2. Proposed decentralized Microgrid control scheme

setpoint SoC^*_H near the maximum SoC, facilitating reaching the maximum SoC as the batteries react more strongly to a voltage drop. In equation (3), $SoC_{\Delta,i}$ is defined for a specific ESS. This definition applies individually to each ESS within the DC Microgrid. Consequently, the variables $SoC_{\Delta,i}$ are used in equations (4) and (5) to reflect the individual state of charge deviations for each ESS. Each $SoC_{\Delta,i}$ is determined by each ESS based on its local measurements.

Remark. By utilizing a DC bus voltage proportional to the grid condition, a self-regulation effect analogous to the one present in AC systems is achieved for all resistive loads connected to the DC bus without a converter.

B. Proposed SoG based DC-AC interlink Control

The control method proposed in the present work for regulating the DC-AC interlink is based on a feature-normalized mapping, for which we introduce the following definition:

Definition I (State-of-Grid)**.** The State-of-Grid (SoG) is a representative quantity for DC and AC Microgrids gained through a feature-normalized mapping between the two physical quantities. For DC Microgrids the SoG is defined as:

$$SoG_{DC,i} = SoG^*_{DC} + \frac{SoC_{\Delta,i}}{\sigma} \cdot \left(\frac{V_{DC,i}}{V^*_{DC}} - 1\right) \tag{4}$$

and for AC Microgrids with:

$$SoG_{AC,j} = SoG^*_{AC} + \frac{SoC_{\Delta,j}}{\sigma} \cdot \left(\frac{f_{AC,j}}{f^*_{AC}} - 1\right) \tag{5}$$

with SoG^*_{DC}, SoG^*_{AC} being the desired DC and AC SoG references, $SoC_{\Delta,i}$ as defined in (3), V^*_{DC} and f^*_{AC} representing the nominal reference values for DC voltage and AC frequency, respectively. This definition enables the formulation of grid codes that can naturally be used for both DC and AC Microgrids.
Both $SoG_{DC,i}$ and $SoG_{AC,i}$ are calculated using local measurements obtained from the DC/AC converter. This allows each converter to independently determine these values without the need for communication with other components in the system. Two control approaches based on the SoG are introduced. The first one is a SoG-droop based method, the second one is SoG-PI based control.

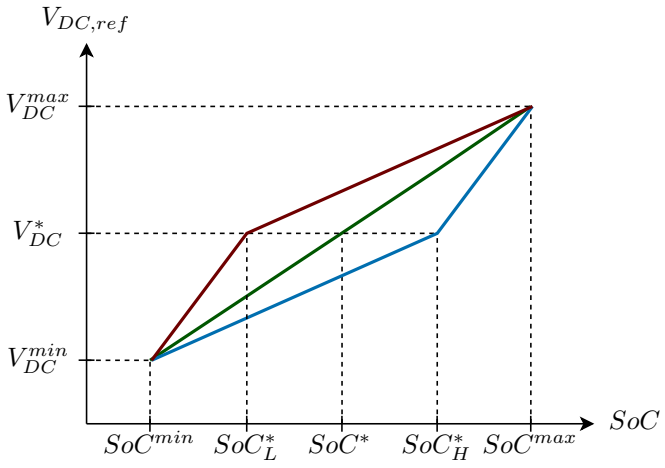

Fig. 3. Examplary Plot of Eq. (1) (3) with SoC^*_L as a low, SoC^*_H a high and SoC^* as a mean SoC setpoint

SoG-difference based: The first approach is based on the difference between the DC side SoG ($SoG_{DC,i}$) and the AC side SoG ($SoG_{AC,j}$), both determined locally by the DC/AC converter, enabling operation without communication. Power converters have an optimal operating range for efficiency. Operating below this range can lead to inefficient operation, resulting in reduced system efficiency [24]. Therefore, requiring a minimum power level helps reducing losses and preventing chattering:

$$P^*_{ij} = \begin{cases} \frac{P^{\max}_{VSC}}{\sigma} \cdot (SoG_{DC,i} - SoG_{AC,j}), & \text{if } |P^*_{ij}| \geq P^{\min}_{VSC}, \\ 0, & \text{otherwise,} \end{cases} \tag{6}$$

with $P^*_{VSC,i} \in [-P^{\max}_{VSC}, P^{\max}_{VSC}]$ being the transferred power from i^{th} DC Microgrid to the j^{th} AC Grid. By using a deadband between $-P^{\min}_{VSC}$ and $P^{\min}_{VSC}$, the function P^*_{ij} is illustrated for $V^*_{DC} = 700$ V, $f^* = 50$ Hz and $P^{\max}_{VSC} = 15$ kW in Fig. 4.

Remark. In the present paper, AC networks are assumed to have a predominantly inductive behavior. For AC networks with resistive characteristics, the approach can be adapted using the voltage based SoG mapping on the AC side to control the active power.

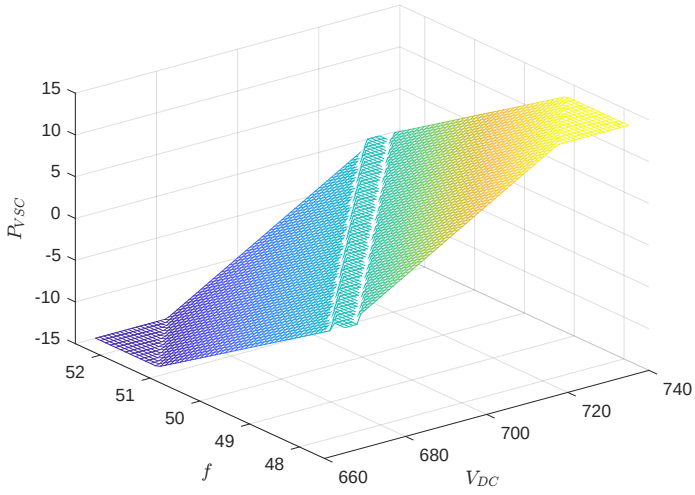

Fig. 4. Examplary Plot of P_{VSC} with $V^*_{DC} = 700$ V, $f^* = 50$ Hz and $P^{\max}_{VSC} = 15$ kW

SOG-PI based: The SoG-difference based approach leads to steady-state errors. By using a PI based control for the VSC,

the control can be expressed with:

$$P_{i,j} = P_{VSC}^{\max} \cdot \phi_i^{\alpha} + P_{tert} \tag{7}$$

$$\phi_i^{\alpha} = \begin{cases} 1, & \text{if } \phi_i \geq 1, \\ -1, & \text{if } \phi_i \leq -1, \\ 0, & \text{if } |\phi_i| \leq \phi^{\min}, \\ \phi_i, & \text{otherwise.} \end{cases}$$

$$\phi_i = -K_{P,i}(SoG_{e,ij}) - K_{I,i} \int_{t_0}^{t} (SoG_{e,ij})\, dx$$

$$SoG_{e,ij} = SoG_{DC,i} - SoG_{AC,j}$$

with ϕ_i^{α} being the saturated and dead-banded control output ϕ_i, $\phi^{\min}$ the factorized minimum power of the VSC, and P_{tert} a optional reference power from tertiary control. A tertiary control is not considered in this paper, therefore $P_{tert} = 0$ in the following.

C. Primary DC voltage & VSC power Control

The reference output voltage $V_{C,Bi}^{*}$ of the battery unit can be controlled by a cascaded P and PI controller, or by a cascaded-PI control as shown in Fig. 5. Each integral control term is saturated and enhanced with an anti-windup. The integral term leads to increased oscillations between the batteries, but removes steady state error. By designing an appropriate gain K_i the oscillations can be reduced significantly.

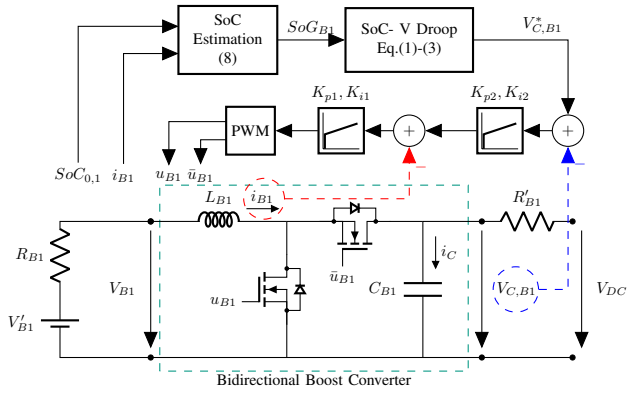

Fig. 5. Control scheme of SoC-V based control with cascaded voltage and current PI and SoC estimation

The power P_{VSC} between the DC and AC side is controlled by a grid-following approach. The reference value $P_{i,j}$ used for this purpose is taken from the presented method (6) for SoG-difference based, (7) for SOG-PI based.

IV. Experimental Setup of the Microgrid

The DC Microgrid configuration employed in this study is depicted in Fig. 1, where a representative electrical equivalent circuit can be found in Fig. 7. The experimental results are obtained from a DC Microgrid experimental setup as depicted in Fig. 6. The laboratory setup includes two battery storage emulators, a PV emulator, passive loads and converter realized by Silicon Carbide (SiC)-MOSFETs (Type: NTHL020N120SC1). The switching frequency is chosen to be 20 kHz. The interlink converter is limited to 10 kW. The

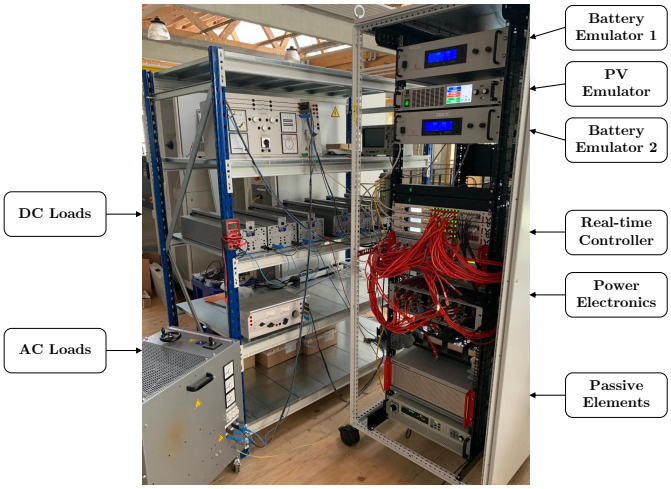

Fig. 6. DC Microgrid experimental setup consisting of PV emulator, loads, Real-time controller, SiC-MOSFETs, passive components and battery emulator

Microgrid parameters corresponding to Fig. 7 are listed in Tab. II. For each parameter, the values are provided in the last column of its row. Additionally, the Voltage Source Converter (VSC) DC side is considered as the point of common coupling.

TABLE II
Circuit Parameters of the Experimental Microgrid Setup

Battery 1	Battery 2	PV	Load 1	Load 2	Value
R_{B1}	R_{B2}	R_{PV}	$R_{L,Ld1}$	$R_{L,Ld2}$	0.1 Ω
C_{B1}	C_{B2}	C_{PV}	$C_{L,Ld1}$	$C_{L,Ld2}$	500 µF
R'_{B1}	R'_{B2}	R'_{PV}	R'_{Ld1}	R'_{Ld2}	0.1 Ω
L_{B1}	L_{B2}	L_{PV}	L_{Ld1}	L_{Ld2}	2.5 mH
R_{01}	R_{02}	R_{03}	R_{04}	R_{05}	10 mΩ

A. Battery Energy Storages

The SoC estimation is based on the Coulomb counting method [25]:

$$SoC_i(t) = SoC_{0,i} - \frac{1}{C_i} \int_{t_0}^{t} I_{Bi}\, dt \tag{8}$$

where $SoC_{0,i}$ is the initial SoC, C_i is the capacity and I_{Bi} is the current of the interfacing converter of battery i. Ageing effects or temperature influences are not considered in this paper. The BESS are emulated by a bidirectional power amplifier with $P_{\max} = 7.5$ kW. The nominal voltages are $V_{B1} = V_{B2} = 380$ V and the initial values of SoC are chosen as $SoC_1 = 0.6$ and $SoC_2 = 0.4$.

B. Renewable Energy Sources

The approach presented is applicable to Microgrids with different RES. Due to the significant expansion of photovoltaic, this work considers it as the primary generation within the grid. The PV panels arranged in a string structure are considered as the main generation of RES in the DC Microgrid. By using an incremental conductance algorithm [26], [27], the Maximum Power Point (MPP) is tracked.

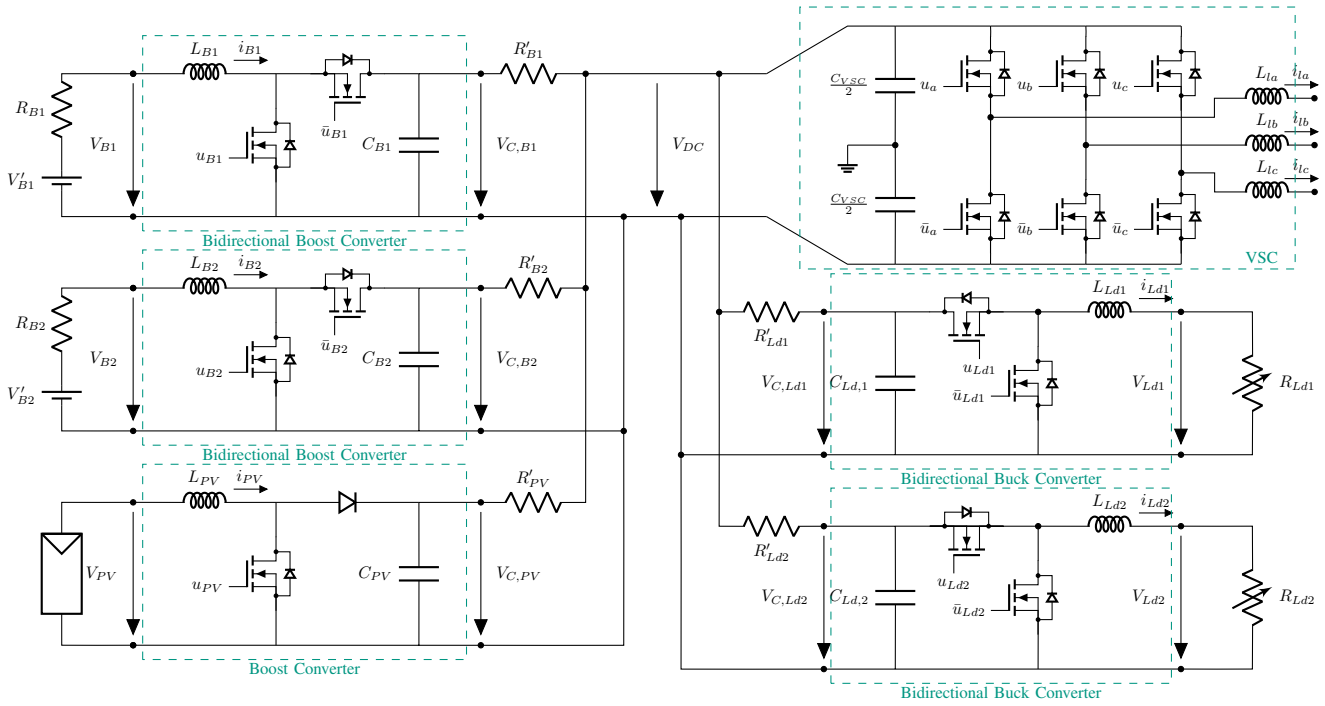

Fig. 7. Electrical circuit of the considered DC Microgrid setup

C. Variable Load Systems

The loads are resistive loads. While resistive loads may not accurately represent the dynamics of all real-world loads, they serve as a reliable and controllable means of testing the stability and performance of the SoG based control. The primary voltage and current regulators are assumed to function adequately. The resistors can be increased or decreased between 0.5 kW and 5.0 kW. The loads are split into two different voltage levels. Devices with a smaller power consumption are connected to a 120 V bus, while larger loads are considered to be connected to a 230 V bus.

D. AC Grid Connection

The DC-AC interlink is a VSC, highlighted in Fig 7, controlled in grid following mode. Each semiconductor of the VSC converter has internal resistors $R_{06} = R_{07} = R_{08} = 10\ \mathrm{m\Omega}$ representing the semiconductor losses. The capacitors of the VSC are $C_{VSC} = 1.5$ mF and the inductors $L_{la} = L_{la} = L_{la} = 2.5$ mH. The nominal power is $P_{VSC}^{\max} = 15$ kW. For the demonstration of the functionality of the presented approach, frequency transitions are required, thus an emulator is employed for AC grid side.

V. Experimental Validation

The results presented in this section aim to demonstrate the effectiveness of the proposed SoG based control approach for DC Microgrids. The validation of the approach is performed in several cases. In Case I, the DC side with two identical batteries is considered in islanded mode. The effects of using two different batteries are examined in Case II, both for the droop based method and the PI based method. The approach for AC-coupled mode with two identical batteries on the DC side is investigated in Case III.

Case I (SoG based droop with identical batteries)**.** The experimental validation of the first approach is conducted by variations in the input, and changes in load. The usable energy is designed to be small ($E_{B1} = E_{B2} = 0.2$ kWh) to conduct significant results within a reasonable time-frame, without compromising the accuracy of the results. This selection does not restrict the functionality of larger batteries. The steps are listed in Tab. III. ΔP_{PV} represents the change in the PV power output in [kW]. ΔP_{Ld1} and ΔP_{Ld2} denote the changes in the power consumed by load 1 and load 2, respectively. Within the test sections, variations in PV power injection may occur, which are attributable to changes in the operating point of the MPPT tracker. However, these variations are insignificant for the experiment and therefore negligible.

TABLE III
Power Steps in Experimental Test

	①	②	③	④	⑤	⑥	⑦
ΔP_{PV}[kW]	0	+3.5	−3.5	+1.5	0	0	+1.5
ΔP_{Ld1}[kW]	0	0	0	0	+2.0	−2.5	0
ΔP_{Ld2}[kW]	0	0	0	0	+0.5	−0.5	0

The results depicted in Fig. 8 demonstrate the effectiveness of the proposed SoG based droop control approach for DC Microgrids. Firstly, the voltage $V_{DC,i}$ of the DC bus remains stable at the determined voltage throughout the experiments, with minor fluctuations observed in response to varying loads and renewable energy generation. This indicates successful regulation of the DC bus voltage within the desired range, ensuring stable operation of the Microgrid. Secondly, the State-of-Charge (SoC) trajectories of individual BESS show

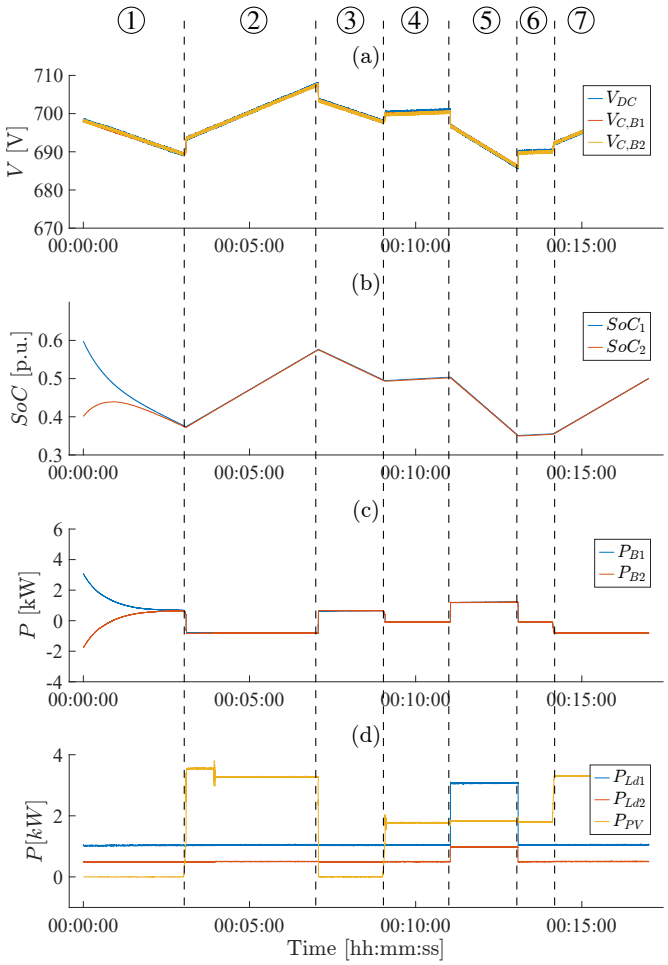

Fig. 8. Experimental results of the proposed SoG based droop control approach for DC Microgrids in islanded mode with two identical batteries. The figure subplots depict the (a) voltage profile of the DC bus, (b) the SoCs of the BESSs, (c) the battery power variations, and (d) the power profiles of the load and PV systems, respectively.

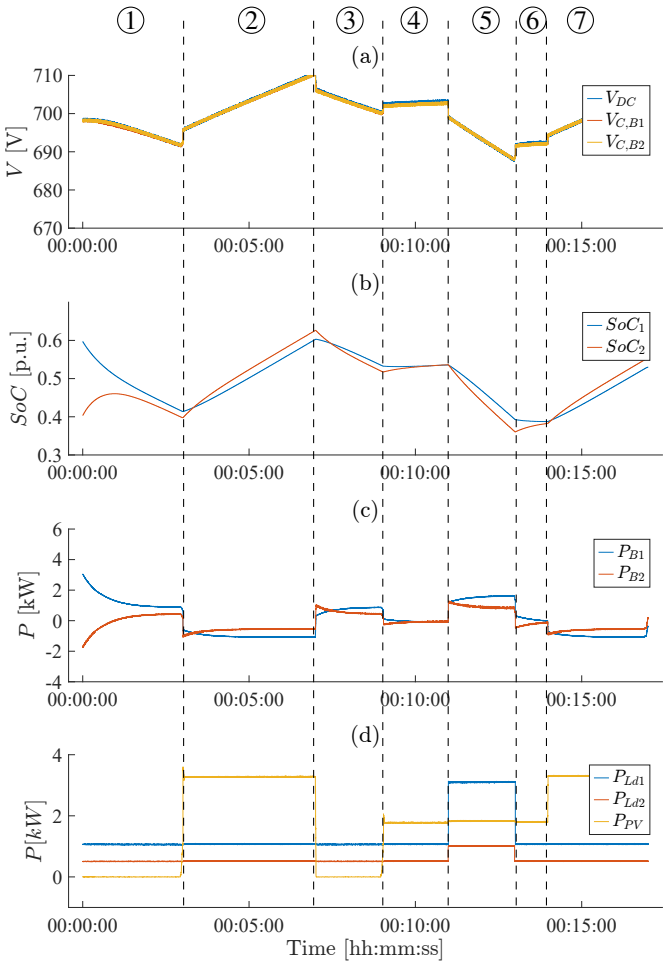

Fig. 9. Experimental results of the proposed SoG based droop control approach for DC Microgrids in islanded mode with two different batteries. The figure subplots depict the (a) voltage profile of the DC bus, (b) the SoCs of the BESSs, (c) the battery power variations, and (d) the power profiles of the load and PV systems, respectively.

effective balancing achieved by the SoG based control strategy. Each BESS unit reaches a similar SoC level over time, indicating successful equalization facilitated by the proposed control approach. Furthermore, both batteries exhibit power sharing capability, dynamically allocating power in response to changes in load demand and the availability of renewable energies. The proposed control method effectively manages battery power fluctuations and optimizes energy utilization within the Microgrid.

Case II (SoG based control with different batteries and line resistances)**.** The variations in input and load consumption used for the investigation of the SoG based approach for different batteries are identical to those in Case I and accordingly listed in Tab. III. The battery 1 is reduced to half its capacity ($E_{B1} = 0.5E_{B2} = 0.1$ kWh). In Fig. 9 the results of a droop based SoG Control is depicted. Compared with the results with two identical batteries shown in Fig. 8, here we observe a divergence of the SoG depending on the load. However, when employing a PI based approach, the differences between the two SoGs are mitigated by the integral component, as depicted in Fig. 10. Nevertheless, the drawback of the PI based method is that it leads to energy oscillation between the batteries during ① and ③. In the case of different batteries, the integral component provides a trade-off between the accuracy of SoC equalization and power oscillations. Additionally, the impact of line resistances on performance was investigated. For this analysis, the line resistance R'_{B1} was increased to 2.5 Ω, corresponding to a line length of 350 m with a cable cross-section of 2.5 mm^2. The results are presented in Fig. 11. It can be observed that the SoC balancing capability is affected; however, unlike conventional droop control, the power balancing capability is maintained after the equalization. In the scenario involving different line resistors, the inclusion of the integral component does not enhance the accuracy of State of Charge (SoC) equalization, unlike its impact in the case of two distinct batteries.

Case III (AC-coupled SoG based Control)**.** The results depicted in Fig. 12 demonstrate the effectiveness of the proposed SoG based control approach for AC-coupled DC Microgrids. While the aspects related to DC side capabilities are similar

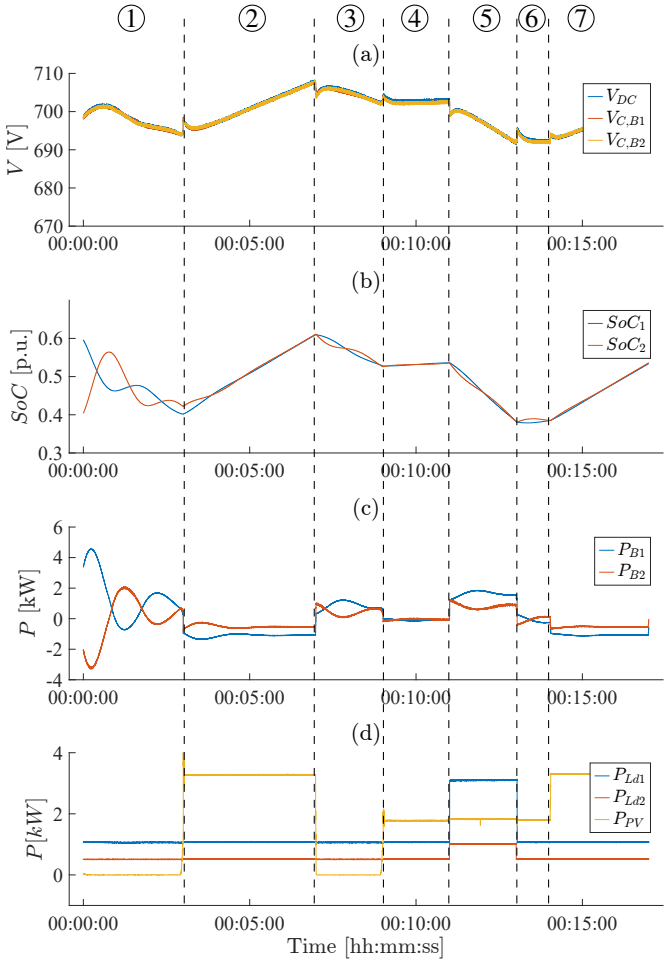

Fig. 10. Experimental results of the proposed SoG based PI control approach for DC Microgrids in islanded mode with two different batteries. The figure subplots depict the (a) voltage profile of the DC bus, (b) the SoCs of the BESSs, (c) the battery power variations, and (d) the power profiles of the load and PV systems, respectively.

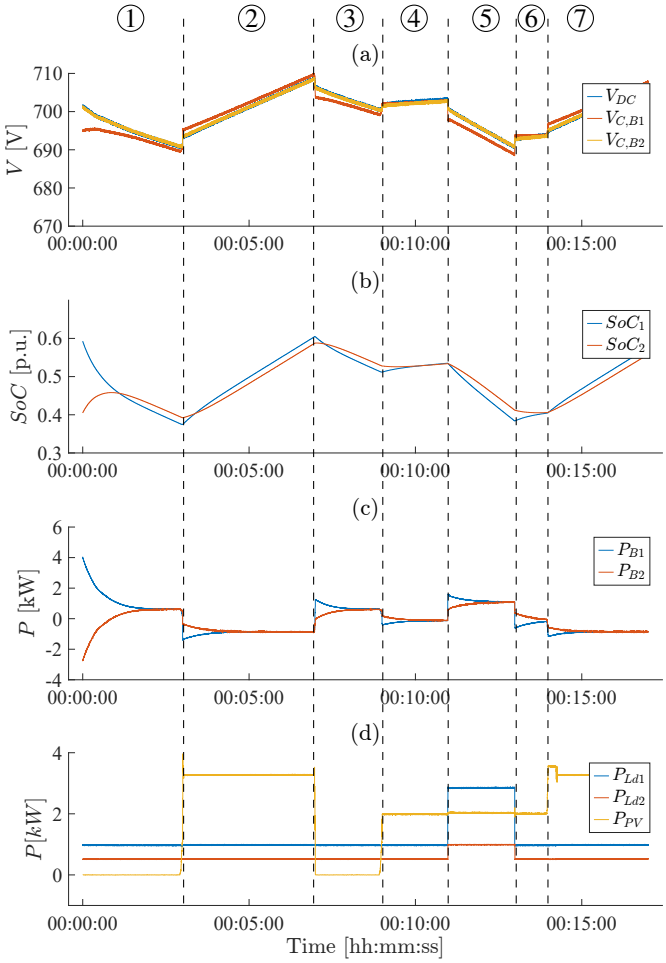

Fig. 11. Experimental results of the proposed SoG based PI control approach for DC Microgrids in islanded mode with different line resistors of the batteries. The figure subplots depict the (a) voltage profile of the DC bus, (b) the SoCs of the BESSs, (c) the battery power variations, and (d) the power profiles of the load and PV systems, respectively.

to those already listed in the previous section, this section highlights the AC interlink insights. The AC grid frequency steps Δf are highlighted in Tab. IV. The VSC dynamically adjusts its active power P_{VSC} output to regulate power flow between the AC and DC side. While during ① the $SoG_{DC,i}$ and $SoG_{AC,j}$ are both around 0.5, the power provided by the VSC remains 0 kW. At step ②, the AC frequency step of 0.5 Hz, which equates a $SoG_{AC,j} = 0.6$, power transfer from the AC side to the DC side is facilitated by the VSC. With increasing $SoCs$ of the batteries, which are leading to increasing $SoG_{DC,i}$, the VSC power decreases. The opposite occurs in ③. In ④, the frequency is set to 50 Hz and the $SoG_{DC,i}$ converges to 0.5. The proposed control approach enables the VSC to maintain grid stability by dynamically adjusting active power exchange based on the SoGs.

TABLE IV
FREQUENCY STEPS IN EXPERIMENTAL TEST

	①	②	③	④
Δf[Hz]	0	+0.5	−1.0	+0.5

VI. CONCLUSION

The present work introduces a novel control method that features communication-free capabilities for SoC balancing and AC coupling. Leveraging the State-of-Grid based control, the proposed approach demonstrates promising results in equalizing the SoC of each ESS throughout DC and AC Microgrids. Through comprehensive simulations and experimental validations, the proposed method shows SoC balancing capability while maintaining load power requirements, regardless of fluctuations in input power, consumption power, or frequency deviations on the AC side, and without the need for any communication. Further advantage of the presented method is the self-regulating effect for resistive loads connected to the DC bus.

REFERENCES

[1] F. Nejabatkhah and Y. W. Li, "Overview of power management strategies of hybrid ac/dc microgrid," *IEEE Transactions on Power Electronics*, vol. 30, DOI 10.1109/TPEL.2014.2384999, no. 12, pp. 7072–7089, 2015.

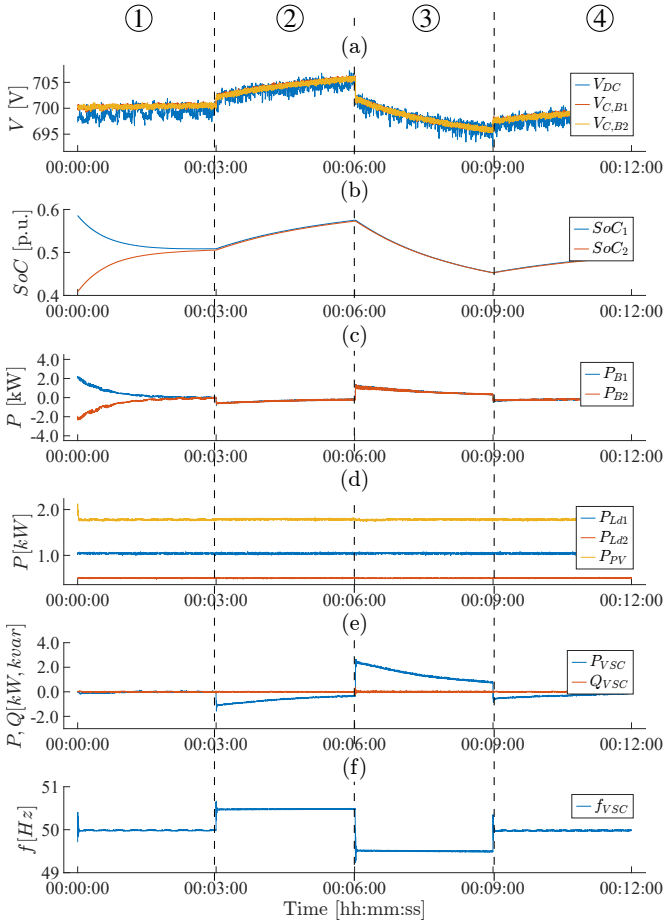

Fig. 12. Experimental results of the proposed SoG based droop control approach for AC-coupled DC Microgrids. The figure subplots depict (a) the voltage profile of the DC bus, (b) the SoCs of the BESSs, (c) the battery power variations, (d) the power profiles of the load and PV systems, (e) the active and reactive power of the VSC, and (f) the AC grid frequency, respectively.

[2] X. Shen, D. Tan, Z. Shuai, and A. Luo, "Control techniques for bidirectional interlinking converters in hybrid microgrids: Leveraging the advantages of both ac and dc," *IEEE Power Electronics Magazine*, vol. 6, DOI 10.1109/MPEL.2019.2925298, no. 3, pp. 39–47, 2019.

[3] B. Zhang, F. Gao, D. Liao, Y. Zhang, and D. Liu, "Distributed ac–dc coupled hierarchical control for vsc-based dc microgrids," *IEEE Transactions on Power Electronics*, vol. 39, DOI 10.1109/TPEL.2023.3335264, no. 2, pp. 2180–2199, 2024.

[4] Y. Yang, Y. Qin, S.-C. Tan, and S. Y. R. Hui, "Efficient improvement of photovoltaic-battery systems in standalone dc microgrids using a local hierarchical control for the battery system," *IEEE Transactions on Power Electronics*, vol. 34, DOI 10.1109/TPEL.2019.2900147, no. 11, pp. 10 796–10 807, 2019.

[5] R. Bhosale, R. Gupta, and V. Agarwal, "A novel control strategy to achieve SOC balancing for batteries in a DC microgrid without droop control," *IEEE Transactions on Industry Applications*, vol. 57, DOI 10.1109/TIA.2021.3073376, no. 4, pp. 4196–4206, 2021.

[6] J. M. Guerrero, J. C. Vasquez, J. Matas, L. G. de Vicuna, and M. Castilla, "Hierarchical control of droop-controlled AC and DC microgrids—a general approach toward standardization," *IEEE Transactions on Industrial Electronics*, vol. 58, DOI 10.1109/TIE.2010.2066534, no. 1, pp. 158–172, 2011.

[7] E. Kabalci and Y. Kabalci, *Smart grids and their communication systems*, no. 1. Springer, 2019.

[8] J. M. Guerrero, J. Matas, L. Garcia de Vicuna, M. Castilla, and J. Miret, "Decentralized control for parallel operation of distributed generation inverters using resistive output impedance," *IEEE Transactions on Industrial Electronics*, vol. 54, DOI 10.1109/TIE.2007.892621, no. 2, pp. 994–1004, 2007.

[9] H. Kakigano, Y. Miura, and T. Ise, "Distribution voltage control for DC microgrids using fuzzy control and gain-scheduling technique," *IEEE Transactions on Power Electronics*, vol. 28, DOI 10.1109/TPEL.2012.2217353, no. 5, pp. 2246–2258, 2013.

[10] X. Lu, K. Sun, J. M. Guerrero, J. C. Vasquez, and L. Huang, "State-of-charge balance using adaptive droop control for distributed energy storage systems in DC microgrid applications," *IEEE Transactions on Industrial Electronics*, vol. 61, DOI 10.1109/TIE.2013.2279374, no. 6, pp. 2804–2815, 2014.

[11] X. Lu, K. Sun, J. Guerrero, J. C. Vasquez, and L. Huang, "Double-quadrant state-of-charge-based droop control method for distributed energy storage systems in autonomous DC microgrids," *IEEE Transactions on Smart Grid*, vol. 6, DOI 10.1109/TSG.2014.2352342, no. 1, pp. 147–157, 2015.

[12] E. K. Belal, D. M. Yehia, and A. M. Azmy, "Adaptive droop control for balancing SOC of distributed batteries in DC microgrids," *IET Generation, Transmission & Distribution*, vol. 13, DOI https://doi.org/10.1049/iet-gtd.2018.6849, no. 20, pp. 4667–4676, 2019. [Online]. Available: https://ietresearch.onlinelibrary.wiley.com/doi/abs/10.1049/iet-gtd.2018.6849

[13] K. D. Hoang and H.-H. Lee, "Accurate power sharing with balanced battery state of charge in distributed DC microgrid," *IEEE Transactions on Industrial Electronics*, vol. 66, DOI 10.1109/TIE.2018.2838107, no. 3, pp. 1883–1893, 2019.

[14] P. C. Loh, D. Li, Y. K. Chai, and F. Blaabjerg, "Autonomous operation of hybrid microgrid with AC and DC subgrids," *IEEE Transactions on Power Electronics*, vol. 28, DOI 10.1109/TPEL.2012.2214792, no. 5, pp. 2214–2223, 2013.

[15] P. Loh, D. Li, Y. K. Chai, and F. Blaabjerg, "Hybrid AC-DC microgrids with energy storages and progressive energy flow tuning," *IEEE Trans. Power Electron.*, vol. 28, DOI 10.1109/TPEL.2012.2210445, pp. 1533–1543, 04 2013.

[16] N. Eghtedarpour and E. Farjah, "Power control and management in a hybrid AC/DC microgrid," *IEEE Transactions on Smart Grid*, vol. 5, DOI 10.1109/TSG.2013.2294275, no. 3, pp. 1494–1505, 2014.

[17] Y. Xia, M. Yu, P. Yang, Y. Peng, and W. Wei, "Generation-storage coordination for islanded DC microgrids dominated by PV generators," *IEEE Transactions on Energy Conversion*, vol. 34, DOI 10.1109/TEC.2018.2860247, no. 1, pp. 130–138, 2019.

[18] M. Nabatirad, R. Razzaghi, and B. Bahrani, "Decentralized voltage regulation and energy management of integrated DC microgrids into AC power systems," *IEEE Journal of Emerging and Selected Topics in Power Electronics*, vol. 9, DOI 10.1109/JESTPE.2020.3034946, no. 2, pp. 1269–1279, 2021.

[19] X. Lin, R. Zamora, and C. A. Baguley, "A fully filter-based decentralized control with state of charge balancing strategy for battery energy storage systems in autonomous DC microgrid applications," *IEEE Access*, vol. 9, DOI 10.1109/ACCESS.2021.3052924, pp. 15 028–15 040, 2021.

[20] J. Su, K. Li, Y. Li, C. Xing, and J. Yu, "A novel state-of-charge-based droop control for battery energy storage systems to support coordinated operation of DC microgrids," *IEEE Journal of Emerging and Selected Topics in Power Electronics*, vol. 11, DOI 10.1109/JESTPE.2022.3149398, no. 1, pp. 312–324, 2023.

[21] N. Hou and Y. Li, "Communication-free power management strategy for the multiple dab-based energy storage system in islanded dc microgrid," *IEEE Transactions on Power Electronics*, vol. 36, DOI 10.1109/TPEL.2020.3019761, no. 4, pp. 4828–4838, 2021.

[22] Z. ye, D. Boroyevich, K. Xing, and F. Lee, "Design of parallel sources in DC distributed power systems by using gain-scheduling technique," in *30th Annual IEEE Power Electronics Specialists Conference. Record. (Cat. No.99CH36321)*, vol. 1, DOI 10.1109/PESC.1999.788997, pp. 161–165 vol.1, 1999.

[23] M. Mosayebi and S. M. Sadeghzadeh, "Nonlinear control analysis of sensors effect and line resistance for current sharing and voltage regulation in DC microgrids," in *2020 10th Smart Grid Conference (SGC)*, DOI 10.1109/SGC52076.2020.9335748, pp. 1–6, 2020.

[24] Ö. Ekin, G. Arena, S. Waczowicz, V. Hagenmeyer, and G. De Carne, "Comparison of four-switch buck-boost and dual active bridge converter for DC microgrid applications," in *2022 IEEE 13th International Symposium on Power Electronics for Distributed Generation Systems (PEDG)*, DOI 10.1109/PEDG54999.2022.9923074, pp. 1–6, 2022.

[25] J. Aylor, A. Thieme, and B. Johnso, "A battery state-of-charge indicator for electric wheelchairs," *IEEE Transactions on Industrial Electronics*, vol. 39, DOI 10.1109/41.161471, no. 5, pp. 398–409, 1992.

[26] D. Sera, L. Mathe, T. Kerekes, S. V. Spataru, and R. Teodorescu, "On the perturb-and-observe and incremental conductance MPPT methods for PV systems," *IEEE Journal of Photovoltaics*, vol. 3, pp. 1070–1078,

2013. [Online]. Available: https://api.semanticscholar.org/CorpusID:41911099

[27] D. C. Huynh and M. W. Dunnigan, "Development and comparison of an improved incremental conductance algorithm for tracking the mpp of a solar PV panel," *IEEE Transactions on Sustainable Energy*, vol. 7, DOI 10.1109/TSTE.2016.2556678, no. 4, pp. 1421–1429, Oct. 2016.